JOURNAL OF APPLIED ELECTROCHEMISTRY **29** (1999) 93–100

Planar oxygen sensor
Part I: Effect of crazing of a zirconia thick film on an alumina substrate

J. GOPAUL, W. C. MASKELL*, K. E. PITT

Energy Technology Centre, Middlesex University, Bounds Green Road, London N11 2NQ, Great Britain

Received 13 February 1998; accepted in revised form 19 May 1998

Thick film amperometric oxygen sensors have been constructed using an ink prepared from a powder of yttria-stabilized cubic zirconia with 150 nm particle size printed onto an alumina substrate. At a fixed temperature these sensors display characteristics typical of an amperometric sensor. However, the limiting current varies with operating temperature (T) according to a $T^{-3.1}$ dependence. This indicates that the diffusion barrier (electrolyte) becomes more restrictive as the temperature is raised. Cracks in the zirconia film (detected by SEM) arise from the differential thermal expansion coefficient of the thick film and the substrate. Diffusion of oxygen to the cathode occurs through the cracks which open and close as the temperature is, respectively, lowered and raised. Measurements at total gas pressures in the range 1–1000 mbar indicate that the mode of diffusion is of the Knudsen-type up to 120 mbar then tending towards mainly a bulk-type at 1000 mbar. Crack dimensions and their relation to the variation of limiting current and temperature dependence for the region of bulk diffusion are treated theoretically. A good correlation with theory is obtained using the results from the two sources, namely, crack dimensions at room temperature and sensor characteristics in the bulk diffusion regime. This provides evidence for the mechanism proposed to explain both the magnitude and sign of the observed temperature coefficient. The value determined by microscopy for the differential coefficient of thermal expansion between the thick film and the substrate (α) was $1.1 \times 10^{-6}\,K^{-1}$. Also, characteristics of the sensor in the bulk diffusion region give a value for α/θ^2 of $0.70 \times 10^{-6}\,K^{-1}$, where θ is the tortuosity factor of the slots. Hence, $\theta = 1.2$. This value is in agreement with the value determined by microscopy within the bounds of experimental uncertainty.

Keywords: *oxygen sensors*, *thick film*, *zirconia*, *amperometric sensors*, *cracks*

List of symbols

D	bulk diffusion coefficient for oxygen ($m^2\,s^{-1}$)
F	faraday constant ($C\,kmol^{-1}$)
I	limiting current (A)
J	molar flux of active species per unit area of substrate ($kmol\,m^{-2}\,s^{-1}$)
k	constant in Equation 4 ($m^2\,s^{-1}\,K^{-1.7}$)
ℓ	electrolyte thickness (m)
M	relative molecular mass of active species ($kg\,kmol^{-1}$)
p_1, p_2	oxygen partial pressure (Pa)
P	total gas pressure (Pa)
Q	mass flux of active species per unit length of slot ($kg\,m^{-1}\,s^{-1}$)
R	molar gas constant ($kJ\,kmol^{-1}\,K^{-1}$)
s	macroscopic length of cracks per unit geometric area of substrate (m^{-1})
S	geometric area of electrode (m^2)
S_1	exposed area of cracks per unit area of substrate; also porosity of the ceramic
T	operating temperature of the sensor (K)
T_1	temperature below which annealing does not occur (K)
X_{O_2}	oxygen mole fraction

Greek symbols

α	differential expansion coefficient between thick film and substrate (K^{-1})
θ	tortuosity factor of the cracks

1. Introduction

Thick film screen-printing technology holds out the prospect of substantial cost reductions compared with most other manufacturing routes for zirconia oxygen gas sensors. However, it does present challenges in materials processing, particularly as the preparation techniques involve relatively high temperature treatments (~1450 °C); operating temperatures are also elevated (~700 °C). Thus, considerable attention must be paid to ink formulations and to drying and firing conditions.

* Author for correspondence.

© 1999 Kluwer Academic Publishers.

Characteristics of sensors prepared using tetragonal zirconia [1, 2] indicated that screen-printed devices did display current–voltage behaviour typical of amperometric sensors [3] with a limiting current directly proportional to the oxygen concentration to which they were exposed. The zirconia thick film was slightly porous (porosity associated with pores connecting the two faces is about 0.03%) and acted both as the electrolyte and the diffusion barrier [2]. Furthermore, grain growth occurring during sintering was shown to be influenced by the purity of the substrate [4], thus indicating the diffusion of impurities, possibly silica, into the thick film during the high temperature treatment.

It was found that the characteristics of sensors made with the tetragonal zirconia depended upon the preparation conditions. Of particular note was the influence of sensor operating temperature on the limiting current at a given oxygen concentration [2, 5]. It is normally desirable that the sensor output be relatively insensitive to temperature as then precise control of temperature is not needed with consequent cost-saving of instrumentation associated with the sensor.

The work reported in this paper had two aims. First, to investigate the possibility of preparing sensors using the cubic form of zirconia. This crystallographic form has a higher ionic conductivity compared with the tetragonal form [6] with the possible benefit of lower sensor operating temperature. Secondly, as an ongoing requirement, to gain an improved understanding of the gaseous diffusion processes taking place in the pores of the thick film. Additional information on this aspect was obtained by construction of a rig to enable the sensors to be operated at total gas pressures from 1 to 1000 mbar. Progress in these areas should result in clarification of the route towards the development of a robust manufacturing process and a sensor less sensitive to preparation conditions and to operating temperature.

2. Experimental details

The principal details for the preparation of inks, thick films and sensors and for instrumentation and test equipment were as previously described [1, 2]. The zirconia powder used was of Japanese origin (Daichi), stabilized in the cubic form with 8 mol% yttria with particle size of about 150 nm. Electrodes (platinum–zirconia cermet) and electrolytes were printed with diameters 4 and 6 mm, respectively. The electrolyte was fired at 1450 °C for 1 h, ramping up to and down from this temperature by 1 °C min^{-1}.

Two sensors, designated 1A and 2A, were made to an identical recipe. The results shown refer to 1A, except for those obtained using the subatmospheric pressure rig. The reason for this is that after determining current–voltage data at atmospheric pressure on sensor 1A the device suffered a fracture due to thermal shock. It (1A) was then examined using scanning electron microscopy (Cambridge Instruments, Stereoscan 240) but clearly it could not provide further information operating as an oxygen sensor.

The rig for operating sensors at total pressures in the range 1–1000 mbar was designed and built. A schematic diagram of this apparatus is shown in Fig. 1. The sensor was heated to its operating temperature using an electrically powered thick film heater [7].

3. Results and discussion

3.1. *Atmospheric pressure and fixed temperature*

Current–voltage curves at 1 bar total pressure and 800 °C are shown for oxygen mole fractions in nitrogen from 1.0 to 21% (Fig. 2). These characteristics are typical of an amperometric sensor, the current rising with increasing applied voltage before reaching a limiting current plateau. The low slopes of the curves in the limiting region indicate that leakage effects other

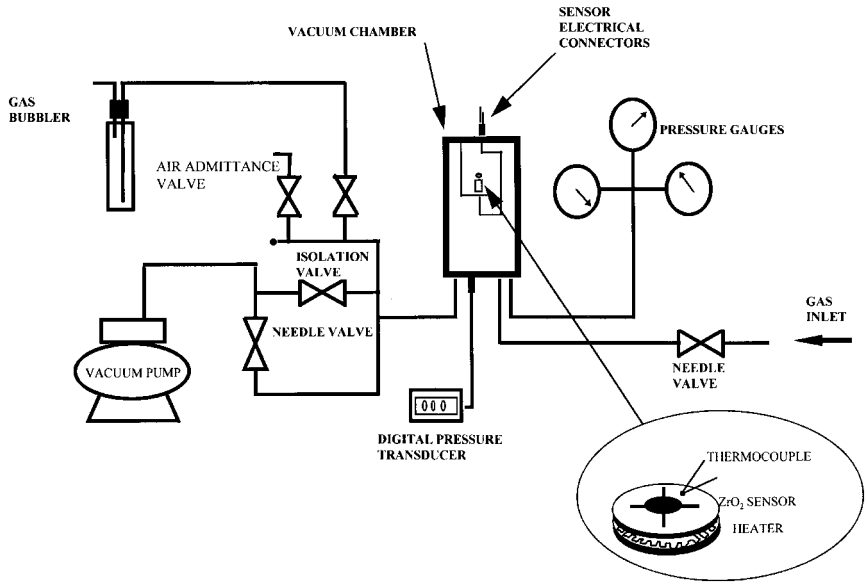

Fig. 1. Schematic diagram of the apparatus for operating sensors in the total gas pressure range 1–1000 mbar and at adjustable gaseous component mole fractions.

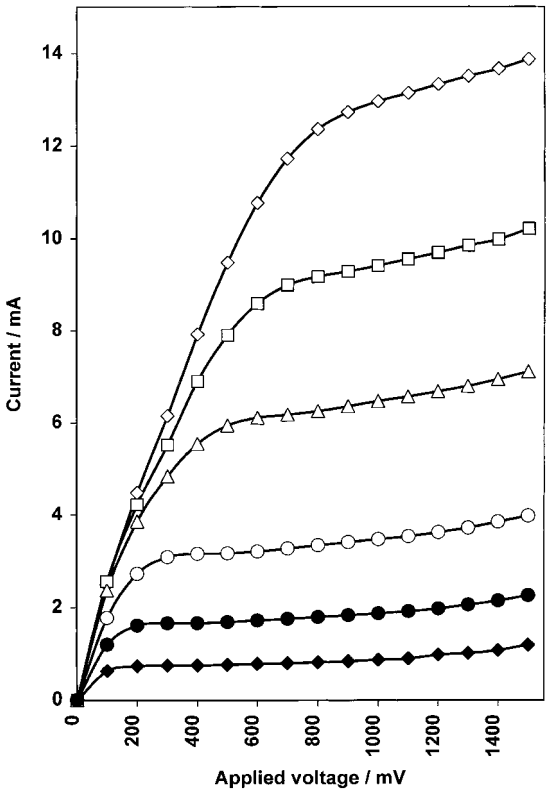

Fig. 2. Current–voltage curves for sensor 1A operated at 1 bar total gas pressure and 800 °C for oxygen mole fractions as follows: (◇) 0.21, (□) 0.15, (△) 0.10, (○) 0.05, (●) 0.025 and (◆) 0.010.

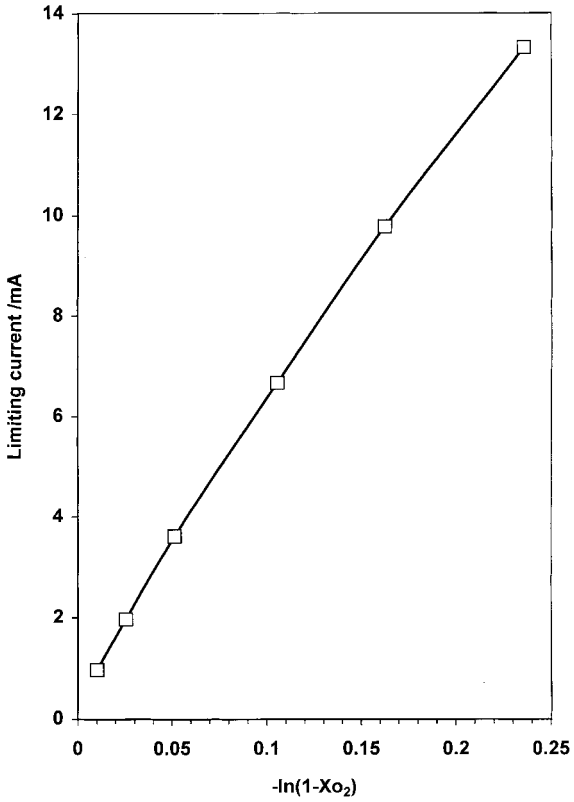

Fig. 3. Limiting current against ln $(1 - X_{O_2})$ for sensor 1A.

than diffusion through the ceramic were not large [8]; at voltages above those shown, the current rose again due to the generation of electronic carriers in the ceramic. The plot of the current against logarithm $(1 - X_{O_2})$ [9], where X_{O_2} is the oxygen mole fraction, is shown in Fig. 3. The results approximated to a straight line; deviations at the higher oxygen concentrations suggest that the currents at 1000 mV had not reached the limiting values as is apparent in Fig. 2. The positive intercept on the current axis is ascribed to a small electrochemical leakage component [8].

3.2. *Atmospheric pressure and variable temperature*

The influence of temperature at a fixed oxygen mole fraction (2.5%) is shown in Fig. 4. The current–voltage curve in Fig. 4 for operation at 650 °C has a different shape from those relating to higher temperatures; this is because the kinetics of the electrode reaction became slow as the temperature was reduced so that a larger driving voltage became necessary to reach the current plateau where diffusion rather than electrode kinetics controlled the rate of the electrode reaction.

The limiting current decreased as the temperature was raised, approximately according to a $T^{-3.1}$ dependence (Fig. 5). This is in general agreement with the behaviour noted recently for a sensor prepared using an ink incorporating the tetragonal form of zirconia [5]; the correspondence suggests that the mechanism in the two cases was probably the same.

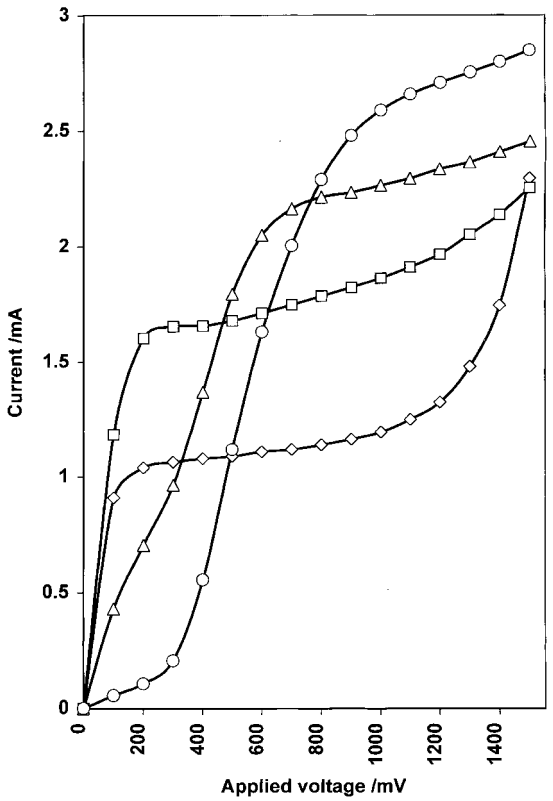

Fig. 4. Current–voltage curves for sensor 1A in 2.5 mol % oxygen at 1 bar total pressure and temperatures as follows: (○) 650, (△) 700, (□) 800 and (◇) 900 °C.

As pointed out previously, dependences of $T^{0.7}$ and $T^{-0.5}$ would be expected for simple bulk- and Knudsen-type diffusion, respectively. The sign is

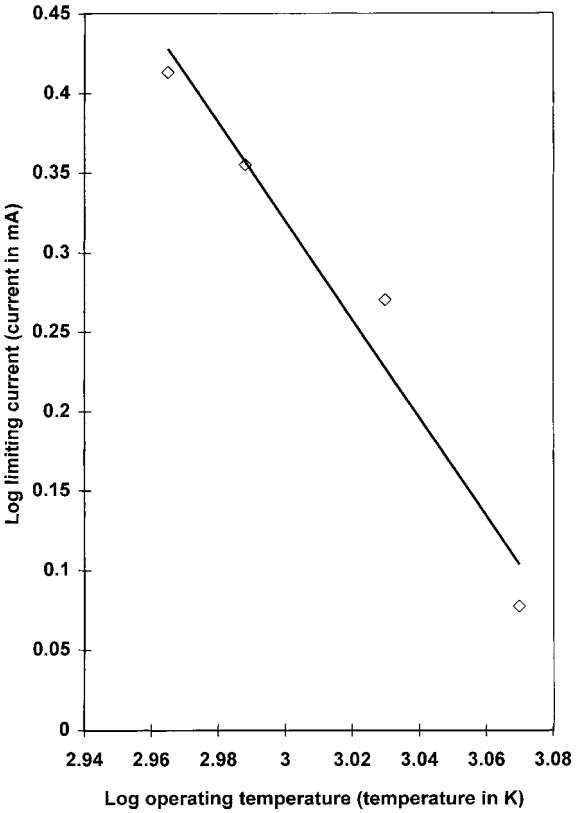

Fig. 5. Variation of limiting current with temperature for sensor 1A indicating a $T^{-3.1}$ dependence.

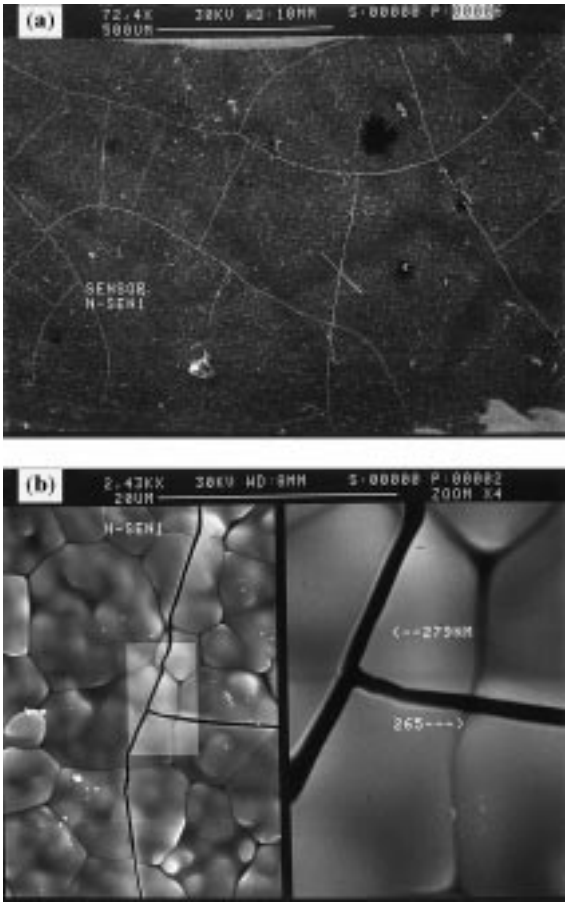

Fig. 6. Micrographs of the surface of sensor 1A: (a) at low and (b) at higher magnification. Bars indicate 500 and 20 μm, respectively.

correct but the magnitude of the dependence is too high to be explained simply in terms of diffusion via the latter mode.

The limiting current in the plateau is controlled by the rate of diffusion of oxygen through the porous electrolyte. The observed variation in the current with temperature would indicate that the barrier was becoming more restrictive to diffusion as the temperature was raised. To gain an insight into this unexpected phenomenon structural studies of the electrolyte were undertaken as described below.

3.3. *Scanning electron microscopy*

Micrographs of both the sensor surface and the fracture edge are shown in Figs 6 and 7. These show the cracking of the thick film. This had not been anticipated but arose as a result of the differing thermal expansion coefficients of the alumina substrate ($\sim 7 \times 10^{-6}\,K^{-1}$) and of the zirconia thick film ($\sim 10.5 \times 10^{-6}\,K^{-1}$) [10] indicating a differential expansion coefficient of approximately $3.5 \times 10^{-6}\,K^{-1}$. The thick film was sintered at 1450 °C and on cooling towards room temperature experienced a tensile stress, resulting in the cracking of the thick film. It would be expected that, having developed, the cracks would open and close as the temperature of the sensor was, respectively, lowered and raised.

This resulted in the hypothesis that diffusion of oxygen to the cathode occurred along the cracks in the electrolyte so that the limiting current decreased as the temperature was raised due to closing of the cracks and vice versa. This hypothesis is tested, as described below, by assuming that, apart from the cracks, the ceramic had negligible porosity connecting the two faces.

The exposed area of the cracks can be related to the differential expansion coefficient, α, between the substrate and the thick film. It is readily shown that the exposed area of the cracks per unit area of the substrate, S_1, is given by

$$S_1 = 2\alpha(T_1 - T) \qquad (1)$$

where T is the temperature at which the crack area was measured or at which the sensor was tested and T_1 is the temperature below which the film did not anneal. This means that the film went into tension below T_1 and could then begin to crack to relieve the stress with further reduction of the temperature. Detailed measurements were made at room temperature of the dimensions of the cracks shown in Fig. 6 both of length and width. These measurements could not be made in the area covered by the electrode as cracks in this region were not visible. The assumption is made subsequently that cracking under the electrode in this work was not significantly different, quantitatively, from that which was not so masked.

The sample examined by scanning electron microscopy comprised half of a complete sensor as the fracture occurred approximately across a diameter.

Table 1. Values of α/θ^2 and θ obtained from the measurements

Technique	θ	$\alpha\theta^{-2}/10^{-6}\,K^{-1}$
Microscopy	$1.1_0 \pm 0.0_5$	$0.8_8 \pm 0.1_0^{*\dagger}$
Limiting current at 1000 mbar total pressure (bulk diffusion region)	$1.2_3 \pm 0.1_5^{*}$	$0.7_0 \pm 0.1_0$

* $\alpha = (1.0_6 \pm 0.01_0) \times 10^{-6}\,K^{-1}$ (determined by microscopy together with the value for T_1 below).
† $T_1 = 1343 \pm 50\,K$ (determined from limiting current against temperature characteristics where bulk diffusion was operative).

The cracks in the whole of the exposed electrolyte were surveyed for length and width. More than 90% of the area conveniently encompassed five squares each of side 1 mm.

Results of the detailed measurements of the cracks are summarized as a histogram (Fig. 8). Cracks had widths mainly in the range 250–350 nm width at room temperature with a tail indicating a significant fraction of cracks up to 750 nm wide. The total fractional crack area in each of five regions of area 1 mm^2 was calculated. This gave the result 2.2×10^{-3} with a standard deviation of 0.5×10^{-3} (standard error $0.2_2 \times 10^{-3}$). This value can then be substituted into Equation 1 to obtain a value of α if T_1 is known. A value for T_1 obtained later from the analysis of the limiting currents in Fig. 11 is 1343 ± 50 K (1070 ± 50 °C); this leads to a value for α of $(1.0_6 \pm 0.1_0) \times 10^{-6}\,K^{-1}$ which is a factor of 3 lower than the value expected from the published individual thermal expansion coefficients of bulk alumina and zirconia.

Measurements were also made of the tortuosity, θ, by measuring the total lengths of cracks running through the thick films from the front face to the substrate by observing the fracture edge using the scanning electron microscope (e.g., Fig. 7). This revealed a value for θ of 1.10 ± 0.05; thus the cracks ran almost normal to the substrate with little meandering.

To formulate a theoretical equation to relate the limiting current and the temperature it is necessary to know the diffusion mode, that is, whether it is bulk or Knudsen diffusion or a mixture of the two. In bulk diffusion the mean free path of the gas molecules is substantially less than the pore size so that collisions between gas molecules are much more frequent than between gas molecules and the walls of the pores of the diffusion barrier. The reverse is the case for Knudsen diffusion where the mean free path is substantially greater than the pore dimensions so that molecule-wall collisions are dominant. A technique to provide information on the diffusion mode is described below.

3.4. *Measurements at total gas pressures below atmospheric*

The mean free path of molecules in the gas increases as the total gas pressure reduces. In fact, the mean free path is inversely proportional to the gas density and, hence, is inversely proportional to total gas pressure and directly proportional to temperature in kelvin; in air at standard temperature and pressure the value is 59 nm [11]. It follows that if the system were operating in the bulk diffusion mode in one region of pressure then reduction of the total pressure could bring about a change to Knudsen mode if pore sizes were appropriate [12].

The diffusion-limited current as a function of total pressure at constant mole fraction of electroactive species provides a test of the diffusion mode operative. In the bulk diffusion mode, on the one hand, the limiting current is independent of the total gas pressure at a given temperature because the product of the diffusion coefficient and the species concentration (in moles per unit volume) is constant. In the Knudsen diffusion region, on the other hand, the limiting current is directly proportional to the total gas pressure at constant mole fraction of the active species. This can therefore be used as a test of the operative diffusion mode as described below.

Measurements at total gas pressures below atmospheric pressure were made using sensor 2A. However, to compare results from 1A and 2A, it was first important to show that the two sensors prepared identically also showed closely similar behaviour. This is demonstrated in Fig. 9. The curvature on the

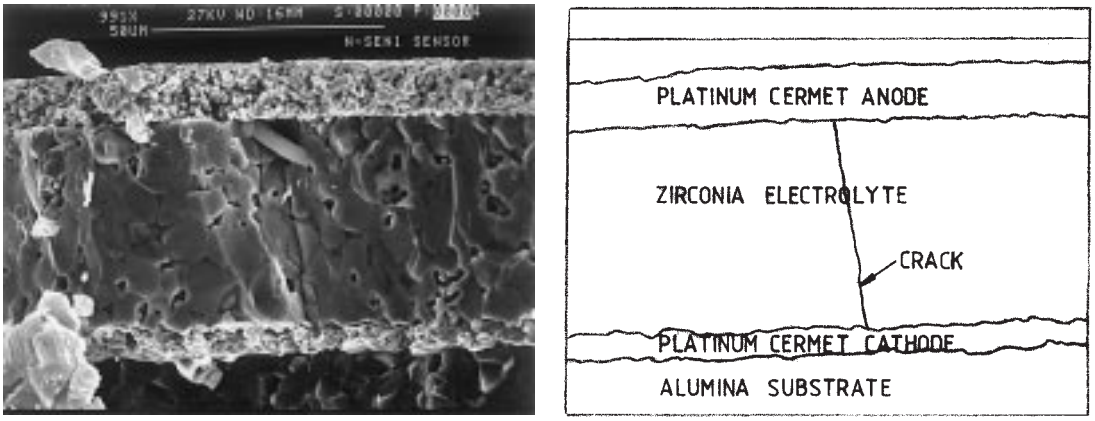

Fig. 7. Micrograph of the fracture edge of sensor 1A. The bar indicates 50 μm.

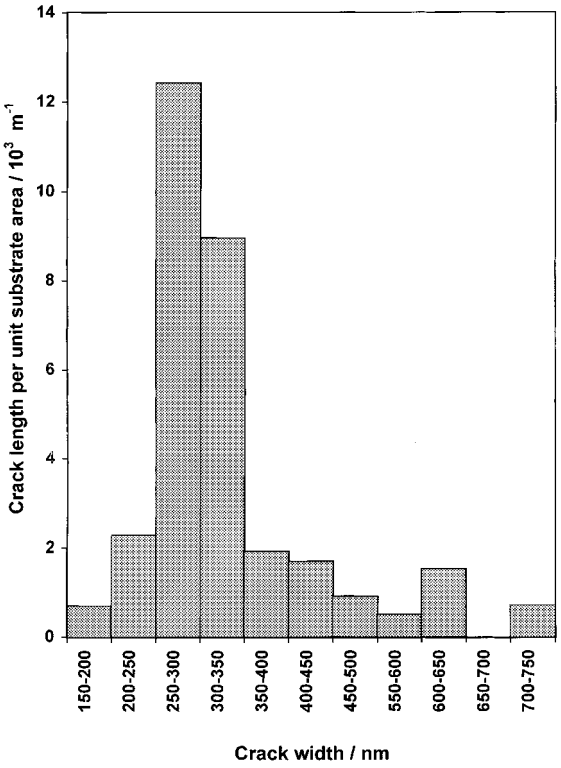

Fig. 8. Histogram indicating the lengths of cracks of given widths, measured at room temperature.

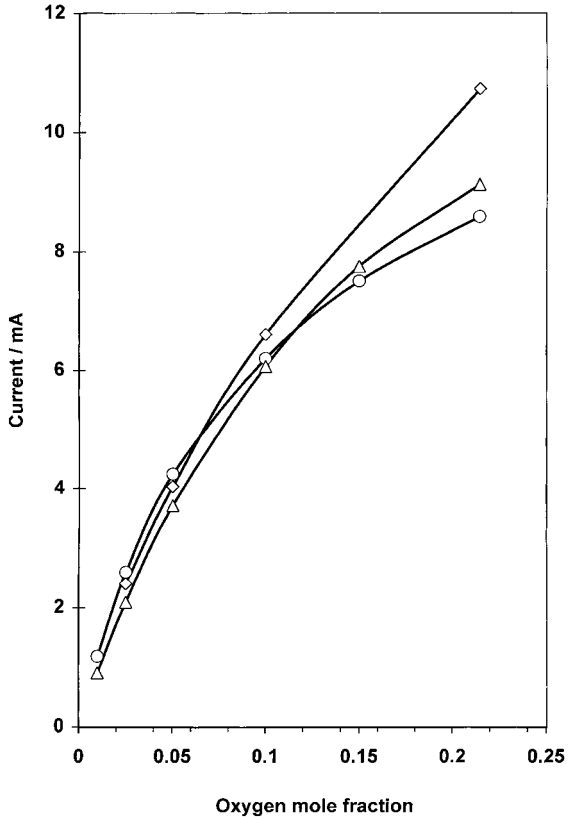

Fig. 9. Current at 1000 mV applied voltage, 1000 mbar total gas pressure and 650 °C operating temperature for sensors 1A and 2A. Symbols: (○) sensor 1A and (△) sensor 2A in the standard furnace; (◇) sensor 2A in the rig shown in Fig. 1.

lines resulted from the low operating temperature of 650 °C at which the sensor was not in the limiting current condition at the higher oxygen concentrations.

Current–pressure characteristics of sensor 2A at pressures below atmospheric are shown in Fig. 10. First, considering the results at pressures up to 120 mbar, the current is directly proportional to total gas pressure in this region. These characteristics are indicative of Knudsen-mode diffusion [12]. Turning now to the results in Fig. 10 for total gas pressures, up to 1 bar, the curves tend towards a plateau with increasing pressure, showing a change in the diffusion mode from Knudsen-type at low pressures towards bulk-type at higher pressures. It is concluded that at atmospheric pressure the principal mode of transport is bulk diffusion, as was implied by plotting the data in the form shown in Fig. 3. Based upon this, the theory that follows assumes bulk diffusion at 1000 mbar total pressure and ignores the small Knudsen component.

A detailed discussion of the results in the Knudsen region is presented elsewhere [13].

3.5. *Analysis of the effect of temperature on sensor characteristics at atmospheric pressure*

Oxygen diffused from the bulk gas to the cathode in the gas phase via the cracks in the zirconia thick film. At the cathode the oxygen was reduced to oxygen ions, O^{2-}, which then migrated in the electric field within the solid electrolyte to the anode where the O^{2-} ions were reconverted to oxygen gas.

The reaction at the cathode is

$$O_2 + 4\,e^- \rightarrow 2\,O^{2-} \tag{2}$$

Equation 2 shows that four faradays of charge are transferred per mole of oxygen diffusing in the gas phase to the cathode. Applying Fick's first law of diffusion and the ideal gas equation to the limiting current situation leads to

$$I = \frac{4FDS_1Sp_1}{RT\ell\theta^2} \tag{3}$$

I is the limiting current, F is the faraday constant, D is the bulk diffusion coefficient of oxygen, S_1 is the observed crack area per unit geometric area of the electrode (note that S_1 is also the porosity of the ceramic representing connected pores between the two electrodes), p_1 is the oxygen partial pressure, S is the geometric electrode area, R is the molar gas constant, T is the operating temperature of the sensor, ℓ is the thickness of the electrolyte and θ is the tortuosity factor of the cracks [14].

For bulk diffusion we can write [15]

$$D = kT^{1.7} \tag{4}$$

where k is a constant for a given species, in this case oxygen. Eliminating D and S_1 from equations (1, 3 and 4) reveals

$$I = \frac{8Fp_1k\alpha S(T_1 - T)T^{0.7}}{R\ell\theta^2} \tag{5}$$

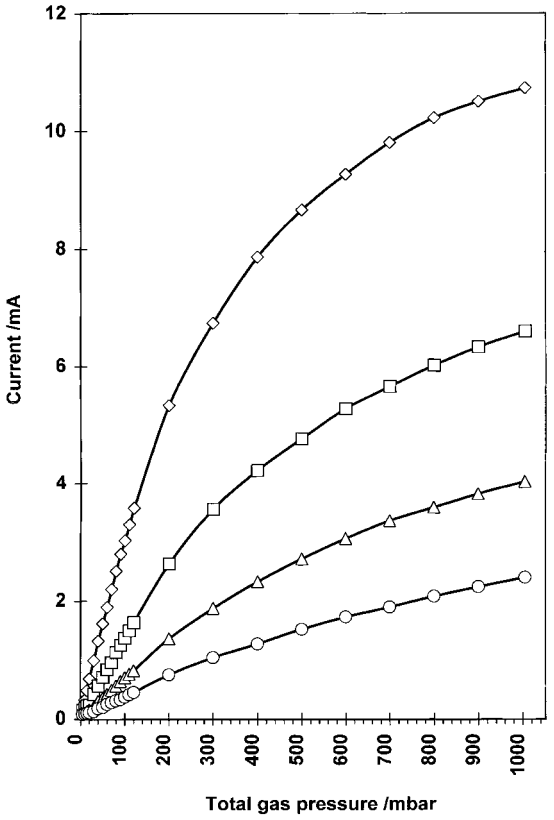

Fig. 10. Current at 1000 mV applied voltage against total gas pressure characteristics of sensor 2A for the pressure range 0–1000 mbar. Oxygen mole fraction: (◇) 0.21, (□) 0.10, (△) 0.05 and (○) 0.025.

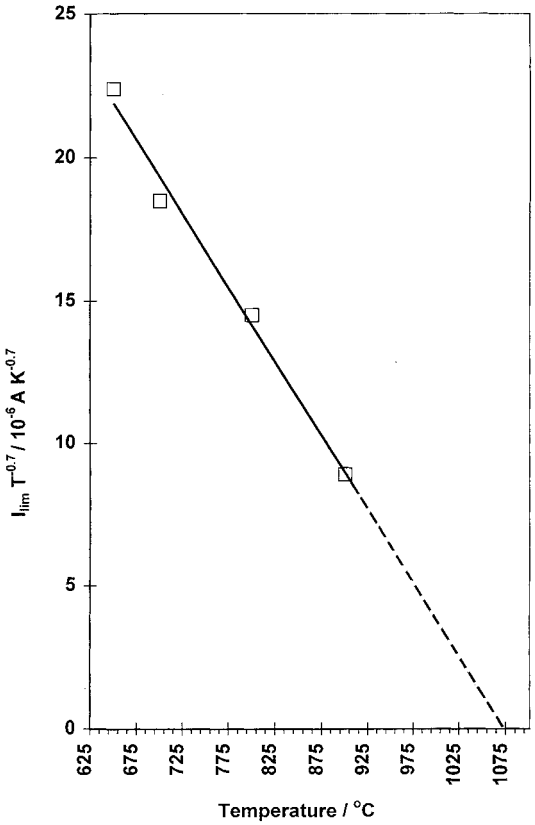

Fig. 11. Plot of $IT^{-0.7}$ against T (see Equation 6).

or

$$IT^{-0.7} = \frac{8Fp_1k\alpha S(T_1 - T)}{R\ell\theta^2} \qquad (6)$$

Thus, a plot of $IT^{-0.7}$ against T should yield a straight line of slope $-8Fp_1k\alpha S/R\ell\theta^2$ and intercept on the T axis, T_1.

The data represented in the above form are presented in Fig. 11 and, within experimental error, do indicate straight line behaviour. The value of k can be determined from a known value for D at a given value of T using equation 4 as follows: $D = 1.7 \times 10^{-4}\,m^2\,s^{-1}$ at 1073 K [16] which leads to $k = 1.2 \times 10^{-9}\,m^2\,s^{-1}\,K^{-1.7}$. The slope $(-54 \times 10^{-9}\,A\,K^{-1.7})$ reveals a value for α/θ^2 of $0.7_0 \times 10^{-6}\,K^{-1}$ (using $R = 8.31\,kJ\,kmol^{-1}\,K^{-1}$, $\ell = 45 \times 10^{-6}\,m$, $F = 96.5 \times 10^6\,A\,s\,kmol^{-1}$, $p_1 = 0.025 \times 10^5\,Pa$, $S = 12.6 \times 10^{-6}\,m^2$); if now the value of α of $1.0_6 \times 10^{-6}\,K^{-1}$ (determined earlier from measurements of cracks, combined with the determined value of T_1) is included, this leads to a value for θ of $1.2_3 \pm 0.1_3$ in satisfactory agreement with that estimated from examination of the cracks in the fracture edge of the electrolyte $(1.1_0 \pm 0.0_5)$.

The intercept on the temperature axis is 1070 ± 50 °C (1343 ± 50 K) indicating that this is the temperature below which the zirconia did not anneal and where the film went into tension and hence became susceptible to cracking. Work on zirconia powders [17] with particle size 0.3 μm has shown that sintering can take place, and hence Zr^{4+} ions are significantly mobile, down to 1180 °C; very small crystallites (~10 nm) showed sintering at 1050 °C providing credence for the value found here (1070 °C).

3.6. *Brief observations*

The quantitative agreement between the results from microscopy and limiting currents is within experimental error providing evidence that the model proposed to explain the observed temperature coefficient of the limiting current, both in terms of magnitude and sign, is generally correct. Furthermore, it would appear that diffusion by routes other than the cracks was negligible and that the ceramic between the cracks effectively had no porosity and hence provided no diffusion path between the two faces.

It is interesting that the value for α determined is a factor of approximately 3 less than that expected from the literature values for the individual components, namely the zirconia thick film and the alumina substrate. This may indicate that regions of thick film between the cracks retained some residual stress.

Results indicate that on cooling from the sintering temperature at a slow rate of temperature change the thick film began to crack at 1070 °C. This would be expected when the temperature was below that allowing annealing of the film to occur. Annealing would cease when the mobility of Zr^{4+} ions became

very small, corresponding to the temperature where sintering effectively ceased.

4. Conclusions

Thick film sensors were prepared using a cubic zirconia powder with particle size 150 nm. The film was sintered at 1450 °C and then cooled slowly back to ambient temperature. Operation at a fixed temperature resulted in current–voltage characteristics, at a total gas pressure of 1 bar, typical of amperometric sensors with a limiting current dependent upon the oxygen mole fraction in which the sensor was immersed. The limiting current was found to be dependent upon the operating temperature with a substantial negative temperature dependence which could not be explained simply in terms of standard diffusion theory.

Examination of the sensor by scanning electron microscopy revealed cracking of the zirconia thick film, the result of a difference in thermal expansion coefficients between the thick film and the alumina substrate onto which it was printed. Detailed measurements of the widths and lengths of the cracks allowed a value for the differential coefficient of thermal expansion of $1.0_6 \times 10^{-6}\,K^{-1}$ to be calculated. It was postulated that the cracks in the film were providing the path for diffusion of the oxygen to the cathode of the sensor. As the temperature of the sensor was raised the cracks closed resulting in reduced diffusion rate and consequently a lower limiting current and vice versa, hence explaining the substantial negative temperature coefficient.

Limiting current measurements were made in the range of total gas pressure from 1 to 1000 mbar. These indicated that up to 120 mbar Knudsen diffusion was operative, while at 1000 mbar the principal mode was bulk diffusion. It was important to establish this in order to develop a testable theoretical framework.

An appropriate plot using the limiting current at 1000 mbar total gas pressure against temperature data revealed a value for α/θ^2 of $0.70 \times 10^{-6}\,K^{-1}$ where α is the differential expansion coefficient of the thick film and substrate and θ is the tortuosity of the pores. Using the α value determined by microscopy led to an θ value of $1.2_3 \pm 0.1_3$ which is in agreement, within experimental error, with the value estimated from examination of the fracture edge of the zirconia by microscopy of $1.1_0 \pm 0.0_5$. The analysis supports the mechanism proposed to explain the temperature coefficient of the limiting current of the sensor observed.

Acknowledgement

The authors thank Professor K. Kendall of Keele University, UK, for kindly providing the Daichi zirconia powder used in this work.

References

[1] A. S. Ioannou and W. C. Maskell, *in* 'Sensors: Technology, Systems and Applications', edited by KTV Grattan (Hilger, Bristol, 1991), pp. 157–61.
[2] A. S. Ioannou and W. C. Maskell, *Solid State Ionics* **53–56** (1992) 85–9.
[3] W. C. Maskell, *J Phys E* **20** (1987) 1156–68.
[4] A. S. Ioannou and W. C. Maskell, *J. Mater. Sci. Lett.* **11** (1992) 1623–25.
[5] A. S. Ioannou, W. C. Maskell and K. E. Pitt, Proceedings of the conference on 'Sensors and their Applications' VIII, Glasgow, 7–10 Sept. 1997, edited by A. T. Augousti andN. White (Institute of Physics, Bristol, 1997), pp. 195–9.
[6] N. Bonanos, R. K. Slotwinski and B. C. H. Steele, *J. Mater. Sci. Lett.* **3** (1984) 245–8.
[7] M. Benammar and W. C. Maskell, *J Phys E* **22** (1989) 933–6.
[8] H. Kaneko, W. C. Maskell and B. C. H. Steele, *Solid State Ionics* **22** (1987) 161–72.
[9] T. Usui, A. Asada, M. Nakazawa and H. Osanai, *J. Electrochem. Soc.* **136** (1989) 534–42.
[10] W. C. Maskell, *in* 'Techniques and Mechanisms in Gas Sensing,' P. T. Mosely, J. O. W. Morris, D. E. Williams, (eds.), (1991), pp. 1–45.
[11] F. H. Newman and V. H. L. Searle, 'The General Properties of Matter', 5th edn, (Arnold, London, 1957), p. 287.
[12] T. Usui, K. Nuri, M. Nakazawa and H. Osanai, *Jpn. J. Appl. Phys.* **26** (1987) L2061–4.
[13] J. Gopaul, W. C. Maskell and K. E. Pitt, Part II of this paper.
[14] J. A. Lee, W. C. Maskell and F. L. Tye, *in* 'Membrane Separation Processes', edited by P Meares (Elsevier, Amsterdam, 1976), pp. 399–476.
[15] R. H. Perry, 'Chemical Engineers Handbook', 6th edn (McGraw-Hill, New York, 1984).
[16] J. O. Hirshfielder, C. F. Curtiss and R. B. Bird, *in* 'The Molecular Theory of Gases and Liquids', (Wiley, New York, 1967), p. 14.
[17] M. A. C. G. van de Graaf and A. J. Burggraaf, 'Advances in Ceramics', Vol. 12, edited by N. Clausen, M. Ruhle and A. H. Heuer (The American Ceramic Society, Columbus, Ohio, 1984), pp. 744–65.